Proceedings of the 17th International Symposium on the
Packaging and Transportation of Radioactive Materials
PATRAM 2013
August 18-23, 2013, San Francisco, CA, USA

Experimental Benchmark of Simulations that Predict Temperatures of an 8x8 Array of Heater Rods within a Vessel Filled with Rarefied Helium Gas

Rachel Green
University of Nevada, Reno
Reno, NV, USA

Ernesto T. Mano
University of Nevada, Reno
Reno, NV, USA

Miles Greiner, Ph.D.
University of Nevada, Reno
Reno, NV, USA
greiner@unr.edu

Jie Li, Ph.D.
Argonne National Laboratory
Argonne, IL, USA

Yung Y. Liu, Sc.D.
Argonne National Laboratory
Argonne, IL, USA

ABSTRACT

A two-dimensional ANSYS/Fluent computational fluid dynamics model is constructed of an existing experiment that consists of a square 8x8 array of heater rods within a square cross section pressure vessel filled with helium. The model includes heat generation and conduction within the rods, conduction and radiation heat transfer across the helium between the rods and enclosure, and the effective thermal resistance at the gas/solid interfaces that is significant at low pressures when the gas is moderately rarified. This configuration is relevant to the vacuum drying process that is used when used nuclear fuel is transferred from underwater to dry storage. Simulations are performed for enclosure temperatures of 27°C and 427°C, and total rod axial heat generation rates between 160 W/m and 820 W/m. Moderately-Rarified simulations, which include an effective thermal resistance between the gas and solid surfaces, are performed for helium pressures of 100 and 400 Pa, thermal accommodation coefficients of 0.25 and 0.4, and a Lennard-Jones collision diameter of 1.9 angstroms. These simulations predict peak heater rod temperatures that are at least 5°C hotter than those predicted by a continuum model, which neglects the rarified gas thermal resistance, when the array heat generation rate is above 330 W/m. Simulations of earlier experiments in the same apparatus, with the helium pressure between 10^5 and $3x10^5$ Pa, predicted peak rod temperatures that were within 5°C of measured values. The current simulation results indicate that the apparatus can be used with a high degree of certainty to benchmark Moderately-Rarified simulation results for rod axial heat generation rates above 330 W/m.

INTRODUCTION

Used light water reactor fuel rods consist primarily of zircaloy cladding tubes that contain highly radioactive fuel pellets as well as high-pressure fission-product and fill gases [1]. The fuel rods are held in a square array by headers, footers and periodic spacer plates. Boiling water

reactor (BWR) assemblies consist of 7x7 to 9x9 rod arrays surrounded by a solid channel. Pressurized water reactor assemblies are 14x14 to 18x18 arrays, but do not have channels.

After being discharged from reactors, used assemblies are stored underwater while their radioactivity and heat generation rate decrease [2]. After sufficient time, typically five years or more, a canister with an internal basket is placed in a transfer cask and lowered into the pool. The canister is then loaded with fuel assemblies, covered, and lifted out of the pool. Helium or another non-oxidizing gas is forced into a port near the top of the canister while water flows out through a tube that reaches to the canister bottom [3]. Small amounts of water may remain at the bottom of the canister and in crevices of the canister and cladding surfaces after draining. Essentially all moisture must be removed from the canister before it is sealed to prevent corrosion of the fuel cladding and cask materials, and/or formation of detonable mixtures of hydrogen and oxygen [4]. After drying, the canister is filled with helium to pressures between 3 and 7 atm (306 to 711 kPa) and sealed either by welding or bolted closure. It is then placed in other packaging for onsite dry cask storage or offsite transport.

With the absence of a defined used-fuel disposal and/or reprocessing path, it is crucial to assure the safety of *long-term* dry cask storage systems [5]. Federal regulations (10CFR72) require that these systems insure that external doses are below certain limits, and that the fuel configuration remains subcritical, confined and contained, and retrievable. The cladding is the primary confinement barrier for the used fuel pellets and fission gas. Its integrity must be protected to assure that, after decades in storage, the assemblies can be safely transferred to other packages, and/or transported to other locations.

Federal regulations (10CFR71) also require that the transport package performance be analyzed under normal conditions of transport (which include a 0.3-m drop) and hypothetical accident conditions (which include a 9-m drop). If the cladding integrity is compromised there is a risk that the fuel will not be in its "as analyzed" configuration after these drop events. Adequate ductility of the cladding must therefore be maintained. Radial hydride formation within the cladding has the potential to radically reduce cladding ductility and its suitability for long term storage or transport [5].

During all post-reactor drying, transfer, storage and transport operations the fuel cladding must be kept below certain temperature limits to avoid (a) dissolution of circumferential hydrides that exist in the cladding and (b) high gas pressures within the tubes, which leads to high cladding hoop stress [6]. If these hydrides dissolve and the hoop stresses become large, then as the heat generation of the used fuel decreases during long-term storage *radial* hydrides may form and cause the cladding to become brittle [7-10]. Drying operations [11] may be the most likely events to cause the fuel temperature to exceed temperature limits. This is because drying is the first operation when the fuel is removed from water and placed in a gas-filled environment, and the fuel heat generation is still relatively high.

Nuclear Regulatory Commission Interim Staff Guidance-11, Revision 3 (ISG-11) [6] specifies conditions that are intended to prevent radial hydride formation. For example, the maximum calculated fuel cladding temperature must remain below 400°C for normal conditions of storage and short term loading conditions (e.g., drying, backfilling with inert gas, and transfer of the cask to the storage pad). For low burnup fuel, a higher short-term temperature limit may be used, provided that the best estimate cladding hoop stress is less than 90 MPa for the temperature limit proposed. During loading operations, repeated temperature cycling is allowed, but is limited to less than 10 cycles with cladding temperature variations of more than 65°C. For off-normal and accident conditions, the maximum cladding temperature should not exceed

570°C, a limit based on creep (stress) rupture consideration. Until further guidance is developed, *high* burnup fuel will be handled on a case-by-case basis [6].

Two methods are currently used by industry for moisture removal from canisters, vacuum drying or forced helium dehydration [3, 6]. In vacuum drying, the canister is evacuated to pressures as low as 67 Pa to promote evaporation and water removal [4]. Several cycles of evacuation and refill may be necessary before operators can demonstrate that the canister is able to meet the drying technical specification of maintaining a low pressure of 400 Pa (3 Torr) for 30 minutes [3, 11].

At the low pressures and gas densities associated with vacuum drying, buoyancy-induced gas motion and natural convection heat transfer from the fuel to the canister surfaces are essentially eliminated. While the gas thermal conductivity is nearly the same at these pressures as it is at atmospheric conditions, the gas is rarefied to the extent that there is a temperature difference (or temperature-jump) between the heated cladding and the gas in contact with it [4, 12-15]. This surface-to-gas temperature-jump is essentially zero at moderate pressures but acts as a thermal resistance between the surfaces and gas at low pressures. These resistances increase the cladding temperature compared to atmospheric pressure conditions. This thermal resistance and the lack of natural convection caused by low pressure may lead to higher cladding temperatures during vacuum drying than during storage conditions for the same fuel heat generation rate.

Forced helium dehydration is used for drying canisters containing high-burnup fuel [3]. In that process, helium is forced into the canister through a port near its top and withdrawn though a tube that reaches to the canister bottom. Moisture is removed from the helium by condensing, demoisturizing, and preheating the gas outside the canister. In some cases cooling water is also circulated in the gap between the canister and transfer cask. The gas pressure during helium dehydration is maintained at roughly the same level as that used during storage. As a result the same natural convection and minimal temperature-jump thermal resistance are expected as in storage. However, gas demoisturizing and cooling equipment are required for forced helium dehydration, which are not needed for vacuum drying.

At the current time, package vendors predict cladding temperatures and hoop stresses during drying using experimentally-benchmark whole-package computational fluid mechanics (CFD) simulations [3, 16]. In these models, the fuel and basket are replaced by a region with an effective thermal conductivity and porosity. This allows prediction of the maximum fuel heat generation rate that can be transferred without exceeding the temperature and hoop stress limits. It also helps determine which fuel may be vacuum-dried, and for which fuel the more complex forced helium dehydration process must be used.

The whole-package computational methods been validated [17] against measurements performed in an actual evacuated storage package [18]. Currently, these effective properties are calculated without regard to the rarefied-gas temperature-jump thermal resistance. However, the fuel heat generation in the tests used to validate the current methods was moderately low. The effect of the rarified-gas thermal resistance on peak cladding temperatures increases with generation rate.

Current Work The long term objective of the current research program is to develop and experimentally-benchmark CFD models of the vacuum drying process that includes the effect of the rarefied-gas thermal resistance. This work will eventually employ an existing experimental apparatus that consists of an 8x8 array of heater rods within an aluminum pressure vessel (Fig. 1). This apparatus simulates a region of a BWR assembly within its channel and between consecutive spacer plates. Experiments will be performed to acquire rod temperatures for a

range of rod heat generation rates, wall temperatures and helium gas pressures. Low pressures relevant to the vacuum drying process will be examined.

In the current paper two-dimensional CFD simulations are performed to model the apparatus filled with helium at 100 and 400 Pa. The simulations include heat generation and conduction within the rods, conduction and radiation heat transfer across the helium-filled region between the rods and enclosure, and the rarified gas thermal resistance at the solid/gas interfaces. The objective is to quantify how much this thermal resistance increases the maximum or peak rod temperature compared to simulations that do not include that effect. These results will be used to determine the experimental conditions under which this effect is sufficiently large that it can be differentiated from random variations in the experimental temperature measurements. In the future the test facility will be used under these conditions to benchmark simulations of drying operations.

EXPERIMENTAL APPARATUS

Figure 1 shows the disassembled test facility that models the region of a used BWR fuel assembly between consecutive spacer plates and within its channel. It was originally constructed to model the thermal conditions during used fuel transport and storage [19, 20]. On the left side of Fig. 1 is an 8x8 square array of rods held by spacer plates at both ends. The rods contain electric heaters and internal thermocouples. The array is placed in a square cross-section anodized-aluminum pressure vessel (right side of Fig. 1). The spacer plates and vessel walls also contain thermocouples. Stainless steel endplates (not shown) are bolted to both ends of the enclosure, and sealed using high-temperature O-rings. The heater power cables and thermocouple lead wires are connected to high-temperature feedthroughs in the endplates. A computer data acquisition system and a power supply are connected to the outer terminals of the feedthroughs to record temperatures and power the heaters.

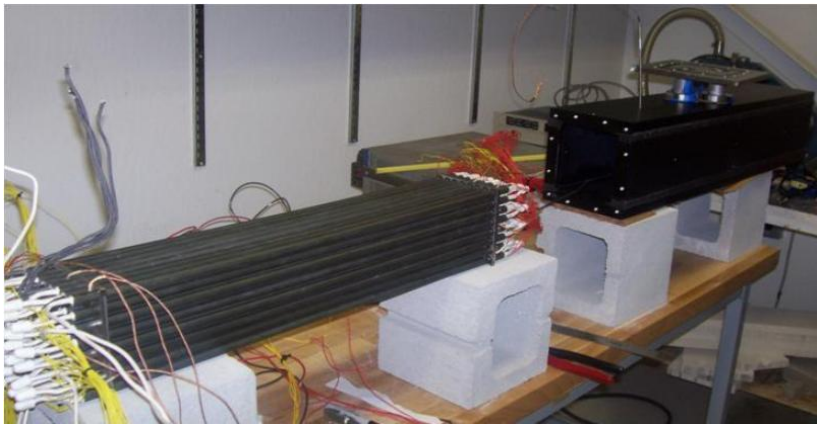

Figure 1. Disassembled view of an experiment apparatus consisting of an 8x8 array of heater rods within a square cross-section aluminum pressure vessel [20]

Each heater rod is 1.1 cm in diameter and has a L = 60.9-cm heated length. Individual heater rods are made up of compressed MgO core surrounded by a 0.7-mm-thick Incoloy sheath. The heaters are arranged in a square pattern with center-to-center pitch spacing of 1.46 cm. The enclosure interior surface is a square, 12 ± 0.25 cm on each side. The array is centered within

the aluminum vacuum chamber. As a result the minimum spacing between the rods and the wall is 3.35 mm, while the minimum spacing between adjacent rods is 3.6 mm.

The heated rod length is shorter than the typical 3.6-m active length of a fuel assembly. As mentioned before, the apparatus is intended to be representative of a region between consecutive grid spacers [1]. The surface emissivity of the rods and chamber walls are 0.8 (specified by the manufacturer) and 0.5 for the anodized aluminum walls [21].

Steady-state rod and surface temperature measurements were made in seventy-two experiments under the following conditions: (a) helium or nitrogen fill gases at pressures of 1 to 3 atm, (b) rods in the vertical (storage) and horizontal (transport) orientation, (c) array heat generation rates of 100 to 500 W, and (d) different thicknesses of insulation surrounding the system (to increase the aluminum enclosure temperature to up to 280°C).

Figure 2a shows the apparatus wrapped in insulation in the vertical orientation. Figure 2b shows heater surface temperature contours calculated from a three-dimensional CFD simulation of the experimental apparatus in the vertical orientation [20]. Half of the heaters are removed to show the hottest rods. This calculation was performed using the ANSYS/Fluent CFD package with the enclosure filled with nitrogen gas at 3 atm. The simulations include heat generation and conduction within the rods, and natural convection and radiation heat transfer across the gas. Figure 2b shows buoyancy-induced gas motion causes the highest temperatures to be above the array center. Simulations with helium (not shown), which has a higher thermal conductivity than nitrogen and so are not as affected by buoyancy, show the maximum temperature is closer to the rod mid-height.

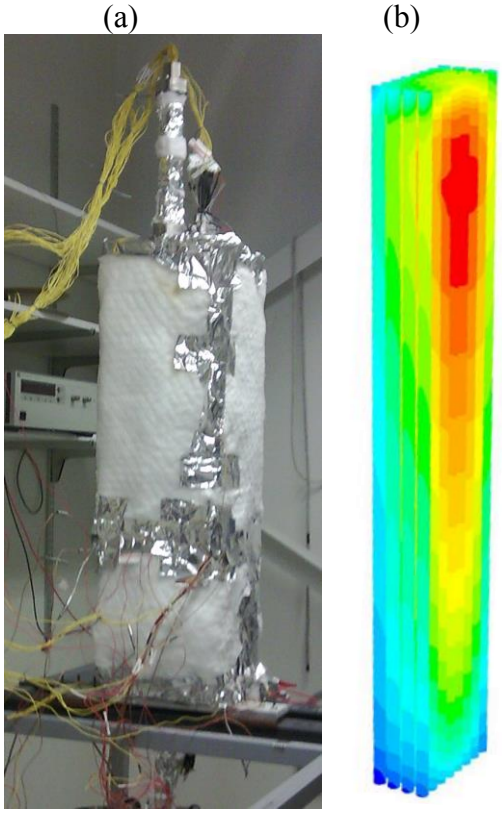

Figure 2. (a) Experimental apparatus in the vertical orientation and wrapped in insulation. (b) Heater surface temperature contours from ANSYS/Fluent simulations. Half of the heaters are removed to show the hottest locations. [20]

Figure 3 shows simulated versus measured results for the temperature difference between the hottest measured rod location and the wall [20]. The results from experiments and simulations are included, for different wall temperatures, heat generation rates, gas pressures, for both helium and nitrogen fill gases. The figure shows that 95% of the simulated temperature differences were within 5°C of the measured data.

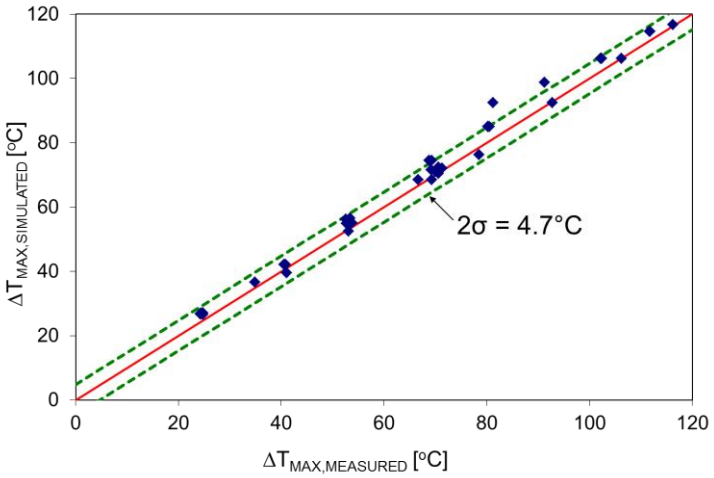

Figure 3. Simulated versus measured results for the difference between the hottest rod and wall temperatures. Results are presented for 42 experiments with different rod heat generation rates, wall temperatures, gas pressures, for both He and N_2 gases. [20]

In the current work we wish to determine if the apparatus described in this section can be used to benchmark rarified-gas simulations under conditions that are relevant to vacuum drying. In order to do that with a high degree of certainty, the experiment must be operated under conditions that cause the maximum temperature predicted by rarified gas simulations to be at least 5°C hotter than simulations that do not include this effect.

RARIFIED GAS HEAT TRANSFER

Under normal atmospheric conditions, gas molecules confined within a moderate-sized volume experience many collisions with each other between interactions with the walls (4, 12-15). The mean free path between molecular collisions is:

$$\lambda = \frac{kT}{\sqrt{2}\pi P d^2} \quad , \qquad (1)$$

where k is the Boltzmann constant, T is the local temperature, P is the local pressure, and d is the Lennard-Jones collision diameter of the molecules.

Knudsen Number (Kn) is the ratio of the mean free path to the characteristic length L_C of the region occupied by the gas:

$$Kn = \frac{\lambda}{L_C} \qquad (2)$$

We note that L_C is easily defined in simple enclosures such as parallel plates, spheres and cylinders. However, in complex geometries such the enclosed heater rod array in Figs. 1 and 2, the characteristic length is not easily determined.

If $\lambda << L_C$, a molecule will experience "many" molecular collisions between interactions with the walls, and the molecules at any location reach equilibrium with each other. As a result when $Kn << 1$, the gas may be treated as a continuum. When $Kn < 0.01$, the Navier-Stokes and Convective Energy equations accurately model momentum and energy transport within a gas [13]. Moreover, at the interface between the gas and solid surfaces, the gas and wall temperatures and their velocities are effectively the same, that is $T_G = T_W$, and $V_G = V_W$ (no-slip boundary condition).

Equations (1) and (2) show that the molecular mean free path and the Knudson number increase as the gas pressure decreases and/or temperature increases. If Kn is sufficiently large then a molecule experiences only a few molecular interaction between wall collisions. Under those conditions, the system exhibits characteristics of a coarse molecular structure, and the gas is considered rarified. When $Kn > 0.1$ the Boltzmann kinetic equation must be applied to accurately model the gas, and its numerical solution is computationally intensive [13].

For $0.01< Kn < 0.1$ the gas is considered to be at a level of slight rarefaction [14]. In such cases the gas tends to behave as a continuum in regions away from the walls. However, a molecule that comes into contact with a wall does not meet other molecules enough times to reach equilibrium with them in the vicinity of the wall [15]. Therefore there can be an abrupt change of temperature and speed from the surface to the gas, that is $T_G \neq T_W$, and $V_G \neq V_W$. This is known as temperature-jump or slip-flow. As a result, for $0.01< Kn < 0.1$, the Navier-Stokes and Convective Energy equations accurately model momentum and energy transport away from the walls, but gas rarefaction must be taken into account at the walls using "temperature-jump" and "velocity-slip" boundary condition [13, 14]. Due to the difference in the gas and surface velocity, this condition is known as the slip-flow regime.

Under moderately rarefied conditions, Sharipov [22] indicates that the local temperature-difference or temperature-jump between the gas and wall is determined using a resistance model,

$$T_G - T_W = R_{TJ} Q \,. \qquad (3)$$

In this model, Q is the portion of the heat transfer rate directed to the solid surface transported by conduction within the surrounding gas and does not include the component transported by radiation to other surfaces. The temperature-jump thermal-resistance is

$$R_{TJ} = \frac{\mu}{P}\left(\frac{2kT_W}{m}\right)^{1/2} \frac{\zeta_T}{A\kappa} \,. \qquad (4)$$

In this expression μ is the gas dynamic viscosity, m is the mass of a gas molecule, κ is the thermal conductivity of the gas, and A is the surface area. The Temperature Jump Coefficient ζ_T

in Equation (4) is determined by applying the Boltzmann Equation to the Knudsen Layer [13], and is calculated as

$$\zeta_T = \frac{2-\alpha}{\alpha}\frac{\sqrt{\pi}\gamma}{(\gamma+1)\mathrm{Pr}}, \text{ where } \mathrm{Pr} = \frac{\mu}{\kappa}c_P . \qquad (5)$$

In these expressions α is the gas/surface accommodation coefficient γ is the gas specific heat ratio, Pr is the gas Prandtl number, and c_P is the gas specific heat at constant pressure.

SIMPLE CONCENTRIC CYLINDER MODEL PROBLEM

Figure 4a shows a two-dimensional ANSYS/Fluent computational mesh of a helium-filled annular-space with inner and outer surface temperatures and radii of, respectively, T_{Wi} = 400°C and r_i = 1 cm, and T_{Wo} = 350°C and r_o = 3 cm. Its height normal to the plane of Fig. 4a is lL = 1 m. The choice of the dimensions and temperatures of this model problem are somewhat arbitrary.

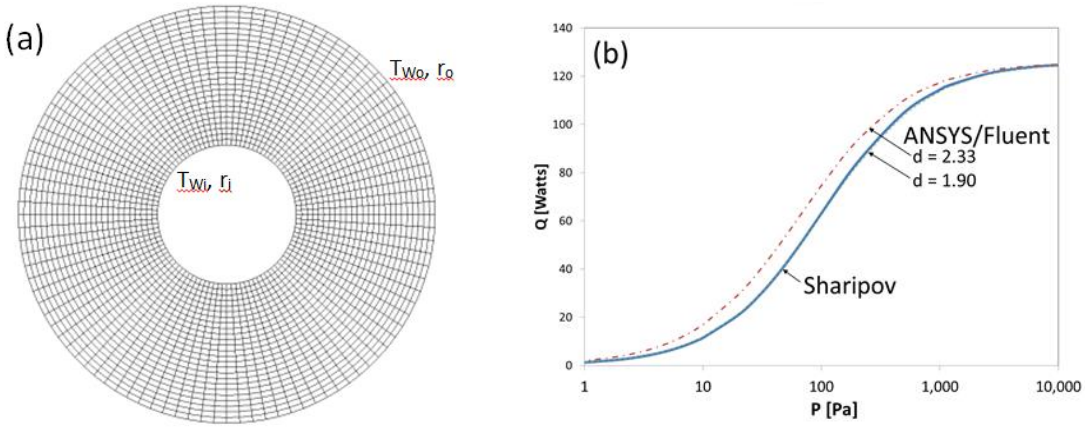

Figure 4. Simple heater rod centered in a cylindrical vessel configuration used to compare ANSYS/Fluent and Sharipov results. (a) Concentric circle computational domain. (b) Heat flux versus helium pressure results from ANSYS/Fluent simulations and Sharpov calculations.

The Sharopov model may be used to predict conduction heat transfer across this region for a range of helium pressures. The heat must flow through a thermal resistances associated with conduction within the helium,

$$R_{COND} = \frac{Ln(r_o/r_i)}{2\pi kL} . \qquad (6)$$

It must also pass through temperature-jump thermal resistances at the inner and outer surfaces, which are respectively

$$R_{TJi} = \frac{\mu}{P}\left(\frac{2kT_{Wi}}{m}\right)^{1/2}\frac{\zeta_T}{2\pi r_i L\kappa} \text{ and } \qquad (7)$$

$$R_{TJo} = \frac{\mu}{P}\left(\frac{2kT_{Wo}}{m}\right)^{1/2}\frac{\zeta_T}{2\pi r_o L\kappa} \quad . \qquad (8)$$

This heat transfer is driven by the temperature difference between the inner and outer surfaces of the annular space. The resulting conduction heat transfer is calculated using a circuit analogy, as

$$Q = \frac{T_{Wi} - T_{Wo}}{R_{TJi} + R_{COND} + R_{TJo}} \quad . \qquad (9)$$

At the average wall temperature of 350°C, the relevant helium properties are $\gamma = 1.666$, $m = 6.642\text{x}10^{-27}$ kg, Pr = 0.68, $\kappa = 0.17$ W/mK, $\mu = 221\text{x}10^{-7}$ Ns/m^2 [23]. When helium is in contact with an "engineering surface" at 27°C and 427°C, the accommodation coefficient is approximately $\alpha = 0.4$ and 0.25, respectively [24].

In Fig. 4b, the solid line marked Sharipov shows the resulting conduction heat transfer versus pressure. For pressures above 10,000 Pa, the heat transfer is essentially the value expected based on conduction in the helium, and the effect of the temperature-jump is negligible. As the pressure decreases below this value, the temperature-jump thermal resistances on the inner and outer surfaces increase, and the heat transfer rate decreases.

ANSYS/Fluent has an option to impose temperature jumps at surfaces due to moderately rarefied gas effects. That model requires specification of Helium's Lennard-Jones collision diameter d. Values of d = 1.9 and 2.33 angstroms are found in the literature [25]. In Fig. 4b, the dashed lines marked ANSYS/Fluent d = 1.9 and d= 2.33 shows heat transfer rate versus pressure for those collision diameters. Like the Sharipov calculation, these heat transfer rates is essentially not affected by gas rarification for P > 10,000 Pa, and decreases due to the increased importance of the temperature jump at lower pressures. The rates predicted with d = 1.9 angstroms are in much better agreement with the Sharipov model than the other value. This value is used in the rest of the simulations presented in this paper.

COMPUTATIONAL MODEL OF EXPERIMENTAL APPARATUS

This section describes the computational methods used to predict the experimental heater rod and helium gas temperatures within the experimental apparatus in Figs. 1 and 2 for a range of isothermal enclosure temperatures T_E, gas pressures P, and rod array heat generation rates Q. Results from Continuum simulations, which do not include temperature jumps between the solid and gas, are compared to those obtained for Moderately Rarified simulations which include the temperature jump. Figure 5 shows a two-dimensional ANSYS/Fluent finite volume grid of the experiment cross section. It includes 64 heater rods, the interior boundary of the enclosure, and the helium gas in-between. Each rod consists of a D = 9.5-mm-diameter magnesium oxide (MgO) core surrounded by a 0.71 mm thick Incoloy sheath. The rod center-to-center pitch is 14.35 mm, and the minimum distance between the rod surface and the enclosure is 1.72 mm. The length of the enclosure walls is 114.83 mm (this is slightly shorter than the experimental apparatus dimension).

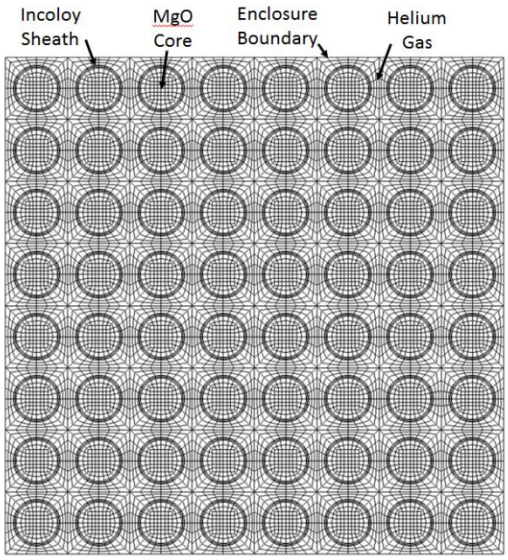

Figure 5. Two-dimensional computational mesh of the experiment cross section composed of 46,592 elements.

The mesh consists of 46,592 elements. The current authors used the same meshing scheme to create a two-dimensional CFD mesh of a 7x7 array with nitrogen at atmospheric pressure, and showed the results were independent of further mesh refinements [26]. Future simulations with the current geometry at low pressures will be performed with different grid refinements to confirm grid independence.

Steady-state thermal simulations were performed using the ANSYS/Fluent package. These simulations included heat generation within the MgO rod cores, conduction within the solids and helium, and surface-to-surface radiation across the helium filled region. These simulations do not include buoyancy-induced gas motion or natural convection in the helium because they are negligible at the low pressures considered in this work. Appropriate temperature-dependent thermal conductivities were applied to each material region.

Simulations are performed with enclosure temperatures of 27°C and 427°C to cover conditions between room temperature and situations that cause the cladding to reaches it limit temperature. Simulations were performed for array heat generation rates between Q = 100 and 500 W. In this work a uniform volumetric heat generation rate applied to the MgO cores that is equal to the total array heat generation rate divided by the MgO volume, $q = Q/(64\pi(D/2)^2L)$. For array heat generation rates between 100 and 500 W and a heated length of L = 60.9 cm, the axial heat generation rates are between 164 W/m and 820 W/m. For a typical BWR with a length of 3.6 m and a peaking factor of 1.25 [1], these axial heat generation rates correspond to assembly heat generation rates between 470 and 2300 W.

Three different heat transfer models are used in this work. The first is the Continuum Model, which does not include temperature jumps between the solid surfaces and the gas. The second is the Moderately-Rarefied Model, which includes the temperature jump thermal resistance described in Equations 4 and 5. Simulations for this model are performed for pressures of P = 100 and 400 Pa, and thermal accommodation coefficients of $\alpha = 0.25$ and 0.4. The last model was for a Hard Vacuum, which neglects all conduction in the helium gas, and assumes all heat transfer between the rods and enclosure is by radiation.

The ANSYS/Fluent package employs a second-order upwind scheme to solve the energy equations. Radiative heat transfer was solved for gray diffuse surfaces using the discrete ordinates method with a second-order upwind scheme. The governing equations were solved using double precision.

RESULTS AND DISCUSSION

Figure 6 shows temperature contours from a Continuum Model simulation with T_E = 27°C (300 K), and Q = 500 W. There is a central high temperature region. The contours exhibit symmetry about horizontal, vertical and diagonal lines, which reflects the symmetry of the geometry and boundary conditions. The maximum or peak temperature in the domain is T_P = 133°C (406 K). Due to symmetry, it appears within all four of the rods closest to the domain center, along the diagonal symmetry lines. The maximum temperature difference within the domain is $T_P - T_E$ = 106°C. Figure 6 shows the s-axis whose origin is at the domain center. It lies on a diagonal symmetry line and passes through four heater rods and a domain corner.

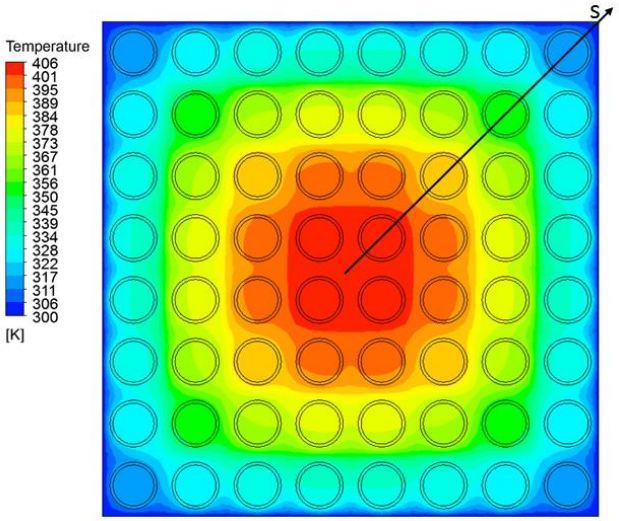

Figure 6. Temperature contours calculated for Q = 500 W, T_E = 27°C, P = 100 Pa and helium gas. The s-coordinate system, whose origin is at the domain center and passes through one corner, is shown.

Figure 7 shows rod and gas temperature minus the enclosure temperature $T - T_W$, versus distance from the domain center along the s-axis for T_E = 27°C and Q = 500 W. Results from Continuum and Moderately-Rarefied simulations are included. The line marked Continuum shows temperatures from the contours in Fig. 6. The temperatures within the four heater rods are relatively uniform compared to the gradients in the gas. Since this model does not include temperature jumps, the gas temperature is the same as the heater rod and enclosure surfaces they it are in contact with.

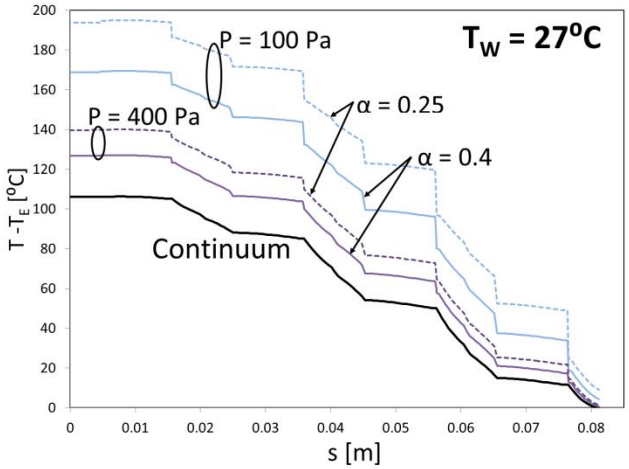

Figure 7. Temperature minus wall temperature along the s-axis shown in Fig. 6, calculated for Q = 500 W, T = 27°C, and helium gas. Results are given for a continuum models (at roughly atmospheric pressure) and low pressured (P = 100 Pa) models with thermal accommodation coefficients of $\alpha = 0.25$ and 0.4.

Moderately Rarified simulations results are also in Fig. 7, for pressures of P = 100 and 400 Pa, and thermal accommodation coefficients of $\alpha = 0.25$ and 0.4. These temperature profiles include thermal resistances between the gas and solid surfaces, which make them hotter than those from the Continuum Model. Equations 3 and 4 show that these resistances increase as P and α decrease. Figure 7 shows that the rod and gas temperature increase as the thermal resistance increase.

The Moderately-Rarified simulation temperature profiles in Fig. 7 exhibit jumps or discontinuities at the interface between the gas and the solid rod and enclosure surfaces. The jumps on the outer surfaces of each rod (the surfaces further from the domain center) increase with distance from the domain surface. This is because the heat flux leaving the rod outer surfaces increases with distance from the center. The effect of the individual temperature jumps accumulate as the distance from the enclosure surface increases. As a result, the differences between the Moderately Rarified and Continuum simulation temperatures are larger at the domain center than they are near the enclosure wall. In each simulation, the peak temperature in the domain, T_P, is located near s = 0.01 m.

Figure 8 shows the maximum temperature difference in the domain, $T_P - T_E$ versus heat generation rate. Results are shown for the Continuum, Moderately-Rarified, and Hard Vacuum simulations. Figures 8a and 8b show results for T = 27 and 427°C, respectively. The peak temperature difference increases with assembly heat generation rate. The Moderately-Rarified results are consistently hotter than the continuum temperatures, and the Hard Vacuum temperatures are hotter still. The temperature differences in Fig. 8b, for the higher enclosure temperature, are smaller than those in Fig. 8a, because the effects of radiation increase with temperature.

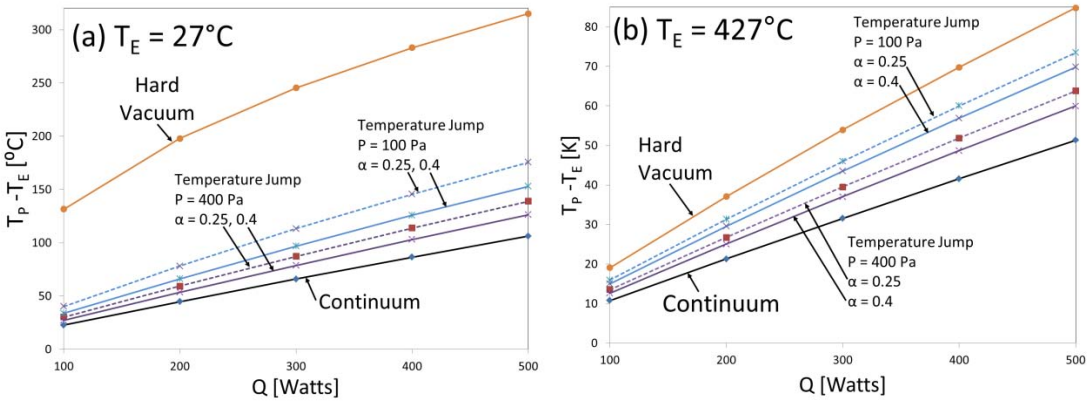

Figure 8. Peak fuel temperature minus wall temperature versus heat generation rate from Continuum, Moderately Rarified (P = 100 and 400 Pa, and α = 0.25 and 0.4), and Hard Vacuum simulation models. (a) T_W = 27°C, (b) T_W = 427°C.

The objective of the current paper is to determine the minimum rod array heat generation rate for which the maximum rod temperatures from the Moderately-Rarified simulations are at least 5°C hotter than those from Continuum calculations. Figure 8 shows that this condition is met if the array heat generation rate is greater than Q = 200 W (axial heat generation rate Q/L = 330 W/m).

SUMMARY

Evacuating helium gas from used nuclear fuel canisters during vacuum drying, to pressures as low as 100 or 400 Pa, has the potential to increase cladding temperatures compared to atmospheric pressure conditions. This is because, at these low pressures, natural convection becomes ineffective at enhancing heat transfer beyond the levels from pure conduction, and the gas become moderately rarified, which effectively increases the thermal resistance between the remaining gas and the solid surface. The overall objective of this research program is to develop and experimentally-benchmark computational models that can be used to predict cladding temperatures during vacuum drying.

In this paper, the Sharipov temperature-jump thermal-resistance model [22] was used to predict the heat transfer across a simple helium-fill annular region as a function of pressure. ANSYS/Fluent simulations of the same configuration were performed with two different Lennard-Jones collision diameters, d = 1.9 and 2.33 angstroms. The simulation with d = 1.9 angstroms exhibited good agreement with the Sharipov calculation. It was therefore used to simulate heat transfer in a square array of heaters rods within an isothermal enclosure. This configuration is relevant to used nuclear fuel assemblies within a canister basket opening. It also models an existing experimental apparatus that has been used to benchmark computational models of used nuclear fuel under storage conditions, in which the helium pressure is between 1 to 3 atm. ANSYS/Fluent simulations of those experiments predicted peak rod temperatures that were within 5°C of the measured value. The objective of the current paper is to determine the heater array heat generation rate for which causes the peak temperature from rarified gas simulations to be at least 5°C hotter than those from continuum calculations.

Two-dimensional ANSYS/Fluent simulations of the experiment cross section were performed for a range of array heat generation rates and enclosure temperatures. Results from

Continuum simulations (which did not include the rarified gas temperature jump) were compared to Moderately-Rarified simulations with at 100 and 400 Pa. When the array heat generation rate was above 200 W, the difference between the peak rod temperatures predicted by the continuum and Moderately-Rarified simulations was greater than 5°C. This indicates that the existing experimental apparatus can be used to benchmark the rarified gas computational models that are being developed to predict used nuclear fuel cladding temperatures under vacuum drying conditions.

FUTURE WORK

The existing experimental apparatus will be used to measure rod temperatures for a range of enclosure temperatures, rod array heat generation rates, and low helium pressures. These data will be compared to results from three-dimensional simulations of the experimental conditions. This comparison will be used to benchmark and/or adjust the computational methods. Computational models of whole transfer packages, in which nuclear fuel is vacuum dried, will be constructed. The effects of gas rarification will be implemented in these models. Steady-state and transient simulations using these models will be performed to predict the peak cladding temperatures. These simulations will be used to develop effective methods for vacuum drying used fuel without causing cladding temperatures that lead to radial hydride formation.

Forced helium dehydration is used to remove moisture from packages containing high burnup and other high-heat-generating fuel assemblies. Vacuum drying these assemblies may cause their cladding temperature to exceed limits that lead to radial hydride formation unless those assemblies spend a very long time in underwater storage pools. In forced helium dehydration, helium is circulated through the canister, and moisture is removed from it by condensing, demoisturizing, and preheating the gas outside the canister. The gas pressure is roughly the same as that used during storage (3–7 atm) so natural convection cooling effects are active, and the gas is not rarified. Future work should consider developing and experimentally benchmarking advanced computational models of forced helium dehydration. To perform that work an enclosed, vertical heater array test facility, whose length is the same as that of a fuel assembly (~3.6 m), with an external circulation system, would need to be constructed. That facility would exhibit the mixed natural/forced convection heat transfer phenomena relevant during forced helium dehydration. These data would be used to experimentally benchmark computational fluid dynamics simulations that can be used to calculate heat and moisture transport during drying operations, and to design efficient drying methods.

After an advanced computational model of natural and forced convection within a canister has been developed and benchmarked for forced helium dehydration, it may be used to solve another difficult problem related to long-term storage of used nuclear fuel. That is, developing a nondestructive method to determine if high-conductivity helium has leaked out of the canister and been replaced by lower-conductivity air [27]. In pressurized vertical storage canisters, buoyancy effects cause the gas in the relatively warm center region to flow upward, and then flow downward near its periphery, i.e., thermal siphoning. Since helium has a relatively high thermal conductivity, the temperatures within the canister and on its external surfaces are relatively uniform. However, if the helium were replaced by air, and since air has a much lower thermal conductivity, the interior and exterior of the canister will exhibit higher temperatures near its top compared to those at its bottom. The advanced computation model of canister convection can be used to calculate the interior and exterior temperatures when helium and air

are within the canister. These results can be used to determine how the external temperature changes if helium were to leak out of the canister, and design method to determine if this has happened by measuring the canister's external temperature.

ACKNOWLEDGMENTS

This work was supported by the US Department of Energy Office of Nuclear Energy's Nuclear Energy University Program.

NOMENCLATURE

BWR	Boiling Water Reactor
CFD	Computational Fluid Dynamics
c_P	Specific Heat [J/kgK]
d	Diameter of the molecules of cover gas [m]
Kn	Knudsen Number [-]
k	Boltzmann constant, 1.38×10^{-23} [m^2kg/s^2K]
L_C	Characteristic Length [m]
m	molecular mass of the gas [kg]
P	Local pressure [Pa]
Pr	Prandtl Number ($C_p\mu/\kappa$)
PWR	Pressurized Water Reactor
Q	Total array heat load [W]
q	Volumemetric heat generation rate [W/m^3]
T_G	Temperature of the gas near the wall [°C]
T_P	Peak or Maximum temperature within domain [°C]
T_W	Temperature of the wall [°C]
T	Local temperature [°C]
α	Thermal accommodation coefficient [-]
ε	Surface emissivity [-]
γ	Specific heat ratio [-]
κ	Thermal conductivity of the gas [W/mK]
λ	Mean free path [m]
μ	Stress viscosity of the gas [kg/ms]
ζ_T	Temperature Jump Coefficient (TJC) [-]

REFERENCES

1. U.S. Dept. of Energy, Office of Civilian Radioactive Waste Management (OCRWM), 1987, "Characteristics of Spent Nuclear Fuel, High-Level Waste, and Other Radioactive Wastes Which May Require Long-Term Isolation", DOE/RW-0184, December.
2. Saling, J.H., and Fentiman, A.W., 2002, *Radioactive Waste Management*, 2nd Edition, Taylor and Francis, New York.
3. Holtec International, "HI-STORM 100 FSAR," Revision 8, Report HI-2002444, 2010.

4. Colmont, D. and Roblin, P., 2008, “Improved thermal modeling of SNF shipping cask drying process using analytical and statistical approaches”, Packaging, Transport, Storage & Security of Radioactive Material, Vol. 19, No. 3, pp. 160-164.
5. Hanson, B., Alsaed, H., Stockman, C., Enos, D., Meyer, R., and Sorenson, K., 2012, “Gap Analysis to Support Extended Storage of Used Nuclear Fuel,” FCRD-USED-2011-000136 Rev. 0, U.S. Department of Energy Used Fuel Disposition Campaign.
6. “Cladding Considerations for the Transportation and Storage of Spent Fuel,” ISG-11 R3, Interim Staff Guidance Report for the Spent Fuel Project Office of the U.S. NRC, 2003.
7. Daum, R.S., Majumdar, S., Liu, Y.Y., and Billone M.C., 2006. “Radial-hydride Embrittlement of High-burnup Zircaloy-4 Fuel Cladding.” J. Nucl. Sci. Tech., Vol. 43, No. 9, Paper 43090, pp. 1-14.
8. Daum, R.S. Majumdar, S., and Billone, M.C. 2008, “Experimental and Analytical Investigation of the Mechanical Behavior of High-Burnup Zircaloy-4 Fuel Cladding.” J. ASTM Intern., Vol. 5, No. 5, Paper ID JAI101209, available online at www.astm.org.
9. Billone, M.C., Burtseva, T.A., and Einziger, R.E., “Ductile-to-brittle transition temperature for high-burnup cladding alloys exposed to simulated drying-storage conditions,” J. Nucl. Mater. 433, 431-448 (2013).
10. Billone, M.C., Burtseva, T.A., and Liu, Y.Y., “Baseline Properties and DBTT of High-Burnup PWR Cladding Alloys,” Proc. PATRAM 2013, San Francisco, CA, August 18-23, 2013.
11. Large, W.S. and Sindelar, R.L., 1997, “Review of Drying Methods for Spent Nuclear Fuel” Westinghouse Savannah River Company, Savannah River Site, Aiken, SC, report number WSRC-TR-0075
12. Pan, L.S., Ng, T.Y., Xu, D., Liu, G.R., and Lam, K.Y, 2002, “Determination of Temperature Jump Coefficient Using the Direct Simulation Monte Carlo Method”, *Journal of Micromechanics and Microengineering*, Vol. 12, pp. 41-52
13. Sharipov, F. and Kalempa, D., 2005, “Velocity Slip and Temperature Jump Coefficients for Gaseous Mixtures. IV. Temperature jump coefficient” *International Journal of Heat and Mass Transfer* 48, pp. 1076-1083
14. Schaaf, S.A. and Chambre, P.L, 1961, *Flow of Rarefied Gases*, Princeton University Press, New Jersey.
15. Loeb, L.B., 1934, *Kinetic Theory of Gases*, 2nd Edition, McGraw-Hill Book Company Inc.
16. Tseng, Y.S, Wang, J.R., Tsai, F.P., Cheng, Y.H., and Shih, C., 2011, “Thermal design investigation of a new tube-type dry-storage system through CFD simulations,” *Annals of Nuclear Energy*, 38, 1088-1097.
17. Holtec International, 2000, “Topical Report on the HI-STAR/HI-STORM Thermal Model and its Benchmarking with Full-Scale Cask Test Data,” Holtec Report No. HI-992252.
18. Pacific Northwest Laboratory, et al., 1987, "The TN-24P PWR Spent Fuel Storage Cask: Testing and Analyses", EPRI NP-5128.
19. Chalasani, N.R., Araya, P., and Greiner, M., 2009, "Benchmark of Computational Fluid Dynamics Simulations using Temperatures Measured within Enclosed Vertical and Horizontal Arrays of Heated Rods," Nuclear Technology., Vol. 167, No. 3, pp. 371-383.
20. Chalasani, N.R and Greiner, M., 2010, “Benchmark of Computational Fluid Dynamics Simulations Using Temperatures Measured Within Enclosed Vertical and Horizontal Arrays of Heated Rods,” PVP2010-25803, Proceedings of the ASME 2010 Pressure Vessels and

Piping Division/K-PVP Conference, PVP2010, July 18-22, 2010, Bellevue, Washington, USA
21. Modest, M.F., 2003, *Radiative Heat Transfer*, 2nd Edition, Academic Press, New York.
22. Sharipov, F., 2004, "Data on the velocity slip and temperature jump coefficients," *Thermal and Mechanical Simulation and Experiments in Micro-Electronics and Micro-Systems*. Proc. 5th Int. Conf. EuroSimE, Belgium, pp. 243-249.
23. Incropera, F.P. and DeWitt, D.P., 1996, *Introduction to Heat Transfer*, 3rd Edition, J. Wiley & Sons, New York.
24. Song, S., and Yovanovich, M. M., "Correlation of thermal accommodation coefficient for 'engineering' surfaces," *Fundamentals of conduction and recent developments in contact resistance*, Proceedings of the Twenty-fourth ASME National Heat Transfer Conference and Exhibition, Pittsburgh, PA, Aug. 9-12, pp. 107-116.
25. Hirschfelder, J.O., Curtis, C.F., and Bird, R., 1954, *Molecular Theory of Gases and Liquids*, John Wiley & Sons, Inc., p. 552.
26. Araya, P.E. and Greiner, M., 2007, "Two-Dimensional Simulations of Natural Convection/Radiation Heat Transfer for BWR Assembly within Isothermal Enclosure," *Packaging, Transport, Storage and Security of Radioactive Material*, Vol. 18, No 3, pp. 171-179.
27. Tsai, H.C., Liu, Y.Y. and Shuler, J.M., "Monitoring Critical Facilities by using Advanced RF Devices," Proc 15th Intl. Conf. on Environmental Remediation and Radioactive Waste Management, ICEM2013, September 8–12, 2013, Brussels, Belgium.